Fractional Order Modeling and Control of an Articulated Robotic Arm

Sabir Husnain
Department of Mechanical, Mechatronics & Manufacturing Engineering, University of Engineering & Technology Lahore, Pakistan
sabirhasnain577@gmail.com

Rasheed Abdulkader
Department of Electrical Engineering, Imam Mohammad Ibn Saud Islamic University (IMSIU), Saudi Arabia
rmabdulkader@imamu.edu.sa (corresponding author)

Received: 11 August 2023 | Revised: 4 September 2023 and 20 September2023 | Accepted: 29 September 2023

Licensed under a CC-BY 4.0 license | Copyright (c) by the authors | *DOI: https://doi.org/10.48084/etasr.6270*

ABSTRACT

This paper presents a fractional order system modeling of a robotic arm and the development of a Fractional Order PID (FOPID) controller applied to the system. The controller technique originated from non-integer calculus, which improves the robotic arm's overall stability and positioning. The robotic arm system is modeled using the non-integer order technique in order to improve system accuracy. Thus, a non-integer order Proportional Integral Derivative (PID) control method is implemented to stabilize the plant positioning. Using MATLAB/Simulink the FOPID controller simulations were confirmed and compared to the Integer Order PID (IOPID) controller for tracking the robotic arm positioning. Simulation outcomes imply that the proposed non-integer controller increases the system stability and position with/without external disturbances being present in the environment.

Keywords-fractional order control; fractional order modeling; robotic arm; articulated manipulator

I. INTRODUCTION

The development of robotic arms is in high demand and has attracted many research studies in academia and the industry, as it has a crucial role in the artificial intelligence integration. It involves many disciplines such control system, sensor technology, communication technology, and artificial intelligence [1]. Nowadays, most industries make use of robotic applications in order to have faster manufacturing, which increases the production line and preserves higher precision and product quality. Articulated robotic arms dominate the global industrial robotics market, accounting for over 50% of all annual installations, as they offer a large operational area and are capable of functioning in a three-dimensional space [2]. The articulated robotic arm application makes use of performing many tasks that are typically complex or can have health effects of humans. These tasks include working in radioactive or contaminated environments, robotic surgery or welding, space exploration, packaging, detecting and disposing bombs, etc. The basis to develop a systematic control for a robotic arm manipulator is implementing the feedback law, which plays a crucial part in eliminating system uncertainty. With the system having a large margin for disturbances and uncertainty, the control design should be able to handle the nonlinear behaviors of the system dynamic coupling [4].

One of the main goals of the development of robots is to build an adaptive and universal machinery to perform tasks and proactively being adaptive to the condition changes. Although conventional robots are able to perform specific tasks with exceptional precision and speed, there are still difficulties in adapting to other more complex tasks as well as being operated in entirely unstructured environments [5]. Also, the greater the complexity of a control algorithm, the more time is needed for its simulation. This makes the task of developing a quick and precise systemic response a challenge [6]. Consequently, there is still ongoing research to improve and overcome these difficulties. One of the main concerns of this study is to develop a simple controller technique, which can provide speed and precision to overcome disturbances.

In the literature, several integer order control methods have been applied for stabilizing and controlling robotic arm systems using integer order modeling, including Sliding Mode Control (SMC) [6][7], Proportional-Integral/Proportional-Integral-Derivative (PI/PID) control [8], Model Predictive Control (MPC), and H-infinity control [9]. Very limited research exists in modeling a robotic arm as a fractional order system and it is still an open problem to investigate and examine the benefits of applying a fractional controller to stabilize the system. Research discoveries on fractional order controllers suggest that they offer superior quality control compared to classical

integer order controllers in particular, when a fractional controller is applied to a fractional order system model [9][10]. This paper introduces a new modeling method of the robotic arm as a fractional order plant in order to obtain the system dynamics more accurately as compared to the classical integer order modeling with the design and implementation of a fractional order controller using the Artificial Bee Colony (ABC) algorithm to improve system stability with and without the presence of disturbances.

II. SYSTEM MODELING

A. Kinematics

To model the dynamics of the 3-DoF (Degrees of Freedom) articulated manipulator kinematics, the model was developed using the Deviant-Hardenberg (DH) method. DH frame assignment for the manipulator is shown in Fig. 1. Figure 1. The DH table shown in Table I explains the geometric relationship between three manipulator links and the world frame according to the assigned frames [11].

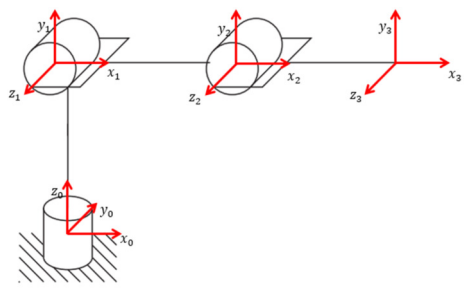

Fig. 1. DH frame arrangement for the articulated manipulator.

TABLE I. DH PARAMETERS OF THE 3DOF ARTICULATED MANIPUALTOR

Joint No.	Joint Rotation (θ)	Link Offset (d)	Link Length (a)	Link Twist (α)
1	q_1	L_1	0	90°
2	q_2	0	L_2	0
3	q_3	0	L_3	0

The transformation matrix is obtained showing the relative position and orientation transform of the end effector with respect to the world frame, which is fixed on the manipulator's base. The transformation matrix is given in (1).

$$T_0^3 = \begin{bmatrix} C_1C_{23} & -C_1S_{23} & S_1 & L_3C_1C_{23} + L_2C_1C_2 \\ S_1C_{23} & -S_1S_{23} & -C_1 & L_3S_1C_{23} + L_2S_1C_2 \\ S_{23} & C_{23} & 0 & L_3S_{23} + L_2S_2 + L_1 \\ 0 & 0 & 0 & 1 \end{bmatrix} \quad (1)$$

hence:

$$p_x = L_3C_1C_{23} + L_2C_1C_2$$
$$p_y = L_3S_1C_{23} + L_2S_1C_2$$
$$p_z = L_3S_{23} + L_2S_2 + L_1$$

B. Dynamics

The dynamic model of the manipulator was obtained using the Euler-Lagrange method, where the Lagrangian provides difference between kinematic and potential energy of the system [12]. This technique is used to obtain the mathematical models of complex system dynamics. The Lagrangian can be used as shown in (2) to get the dynamic model of the manipulator. The Lagrangian is the difference between the total kinetic and the total potential energy of the system $\langle L = K.E - P.E \rangle$.

$$\frac{d}{dt}\left(\frac{\partial L(q,\dot{q})}{\partial q_i}\right) - \frac{\partial L(q,\dot{q})}{\partial q_i} = \tau_i \quad (2)$$

For a system such as the robotic manipulator, the equation can simply be decomposed for simplification, which can ultimately be converted to state space model. The decomposed equation of the manipulator dynamics is shown in (3) obtained by using the Lagrangian method as represented in (2). This non-linear model of the robot is known as the forward dynamics model.

$$T = M(q)\ddot{q} + C(q,\dot{q}) + G(q) \quad (3)$$

where M is the inertia matrix, C is the centripetal or Coriolis matrix, G is the gravity matrix, T is the torque matrix [10][11], and q is a vector containing joint space variables such as the joint angles. The matrices for the 3-DOF articulated manipulator are:

$$M = \begin{bmatrix} M_{11} & M_{12} & M_{13} \\ M_{21} & M_{22} & M_{23} \\ M_{31} & M_{32} & M_{33} \end{bmatrix} \quad C = \begin{bmatrix} C_{11} \\ C_{21} \\ C_{31} \end{bmatrix} \quad G = \begin{bmatrix} G_{11} \\ G_{21} \\ G_{31} \end{bmatrix}$$

where,

$$\left\langle M_{11} = \frac{1}{2}m_1l_1^2 + \frac{1}{3}m_2l_2^2C_2^2 + \frac{1}{3}m_3l_3C_{23}^2 + m_3l_2C_2^2 + m_3l_2l_3C_2C_{23} \right\rangle$$
$$\left\langle M_{22} = \frac{1}{3}m_2l_2^2 + \frac{1}{3}m_3l_3^2 + m_3l_2^2 + m_3l_2l_3C_3 \right\rangle$$
$$\left\langle M_{23} = M_{32} = \frac{1}{3}m_3l_3^2 + m_3l_2^2 + \frac{1}{3}m_3l_2l_3C_3 \right\rangle$$
$$\left\langle M_{33} = \frac{1}{3}m_3l_3^2 \right\rangle$$
$$\langle M_{12} = M_{13} = M_{21} = M_{31} = 0 \rangle$$
$$\left\langle C_{11} = \left[-\frac{4}{3}m_2l_2^2S_{2(2)} - \frac{1}{3}m_3l_3^2S_{2(23)} - m_3l_2l_3S_{2(2)+3}\right]\dot{\theta}_2\dot{\theta}_1 + \left[-\frac{1}{3}m_3l_3^2S_{2(23)} - m_3l_2l_3C_2S_{23}\right]\dot{\theta}_3\dot{\theta}_1 \right\rangle$$
$$\left\langle C_{21} = [-3_3l_2l_3S_3]\dot{\theta}_2\dot{\theta}_3 + \left[-\frac{1}{2}m_3l_2l_3S_3\right]\dot{\theta}_3^2 + \left[\frac{1}{6}m_2l_2S_{2(2)} + \frac{1}{6}m_3l_3^2S_{2(23)} + \frac{1}{2}m_3l_2^2S_{2(2)} + \frac{1}{2}m_3l_2l_3S_{2(2)+3}\right]\dot{\theta}_1^2 \right\rangle$$
$$\left\langle C_{31} = \left[\frac{1}{2}m3\ l_2l_3S_3\right]\dot{\theta}_2^2 + \left[\frac{1}{6}m_3l_3S_{2(23)} + \frac{1}{2}m_3l_2l_3C_2S_{23}\right]\dot{\theta}_1^2 \right\rangle$$
$$\langle G_{11} = 0 \rangle$$
$$\left\langle G_{21} = \frac{1}{2}m_2gl_2C_2 + \frac{1}{2}m_3gl_3C_{23} + m_3gl_2C_2 \right\rangle$$
$$\left\langle G_{31} = \frac{1}{2}m_3gl_3C_{23} \right\rangle$$

C. Fractional Order Model

The dynamic model presented above represents the integer order model for the 3-DoF articulated manipulator. To model it in a fractional order system, its derivatives need to be replaced with fractional order derivatives [12][13].

$$\frac{d}{dt} \rightarrow \frac{d^\gamma}{dt^\gamma} \quad (4)$$

It can be seen that (4) is not right physically, because the dimensions of the integer order derivative are s^{-1} and that of the fractional order is $s^{-\lambda}$. For the sake of consistency, they have to be the same, therefore the following definition is valid [13][14]:

$$\frac{d}{dt} \rightarrow \frac{1}{\sigma^{1-\gamma}} \frac{d^{\gamma}}{dt^{\gamma}} \tag{5}$$

where the parameter σ is arbitrary representing the fractional time component of the system. The time component is known as the cosmic time. Using the dynamic model of the system, the physical relation between order and arbitrary parameter can be approximated as [13]:

$$\gamma = ((inv(MC))^{T} G)^{1/3} \sigma \tag{6}$$

where, due to the fact that the parameter σ incorporates a fractional time component in the system and is used for the existence of physical dimension consistency in the equation, the Plank time constant is also used in research rather than computing it analytically [15].

Now the dynamic model can be represented by replacing the integer order derivative with the fractional order derivative and the equations can be expressed as:

$$T = M(q)\ddot{q} + C(q, \dot{q}) + G(q) \tag{7}$$

where $\ddot{q} = \frac{1}{\sigma^{2(1-\gamma)}} \frac{d^{2\gamma}}{dt^{2\gamma}}$, $\dot{q} = \frac{1}{\sigma^{(1-\gamma)}} \frac{d^{\gamma}}{dt^{\gamma}}$, and $0 < \gamma < 1$.

D. Model Parameters

As the dynamic model was obtained for the dynamic system in analytical form, γ and some other physical parameters such as mass and link lengths are still unknown. The physical parameters of the robot used for this simulation are given as [12]: $m_1 = m_2 = m_3 = 0.5$ kg, $L_1 = 0.15$ m, $L_2 = 0.5$ m, $L_3 = 0.5$ m, and $\gamma = 0.93$.

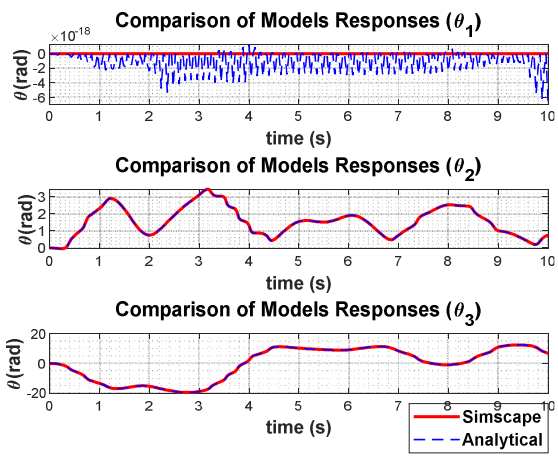

Fig. 2. A comparison of analytical and simscape multibody models.

The order (γ) is obtained by optimizing by employing the ABC genetic algorithm, where γ is tuned by comparing the results with the multibody model of the robot implemented using simscape sim-mechanics. The analytical model parameter is tuned based on the multibody model by minimizing the cost function ITAE $\left(\int t \cdot |e(t)|\, dt\right)$[11]. The result comparison of the analytical and the Simscape model [16] is presented in Figure 2 and the modeling error in the analytical model is shown in Figure 3.

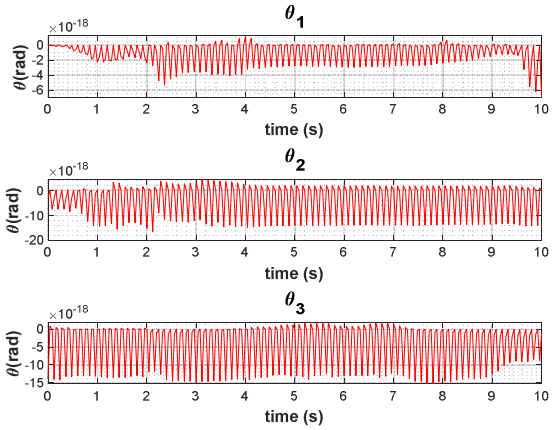

Fig. 3. Modeling error.

III. FRACTIONAL ORDER CONTROL

The controller technique implemented in this research study is a Fractional Order PID (FOPID) controller. For the robotic arm structure, it is crucial for the controller to track the desired position accurately in order to attain a stable operation. Non-integer calculus is a generalized concept to fractional order differential and integral basic operator ${}_aD_t^{\alpha}$ as defined in [17]:

$${}_aD_t^{\beta} = \begin{cases} \frac{d^{\beta}}{dt^{\beta}} & Re(\beta) > 0 \\ 1 & Re(\beta) = 0 \\ \int_a^t (dt)^{-\beta} & Re(\beta) < 0 \end{cases} \tag{8}$$

Non-integer order control design relays on using fractional order exponents of differential and integral operations in the Laplace domain to reach the design requirements that the classical integer order can't achieve, allowing to fulfill a robust constraint performance [5]. Non-integer order PI/PID controllers are proposed as a generalization of integer order PI/PID. Thus, with the fractional order PI/PID controller, additional tunning parameters are added to the controller which improve the overall controller design to meet the system specifications more precisely as compared to the integer order PI/PID controllers [18]. The dynamic model has been developed using fractional calculus, where the fraction order is tuned using the ABC algorithm. Now, a control system can be designed to control the manipulator state in the task space where feedforward control with FoPID controller is used. For that, an inverse dynamic model is used as a feedforward network in the controller which can be obtained by utilizing the dynamic model of the robot manipulator where the equation of inverse dynamic model will be:

$$M(q)^{-1}[T - C(q, \dot{q}) - G(q)] = \ddot{q} \tag{9}$$

where $\ddot{q} = \frac{1}{\sigma^{2(1-\gamma)}} \frac{d^{2\gamma}}{dt^{2\gamma}}$ $\dot{q} = \frac{1}{\sigma^{(1-\gamma)}} \frac{d^{\gamma}}{dt^{\gamma}}$, and $0 < \gamma < 1$, which can then be simplified as:

$$\int\int M(q)^{-1}[T - C(q,\dot{q}) - G(q)] = q \qquad (10)$$

The inverse dynamic model of the system will accept position, velocity, and acceleration states in task space and compute the output in the form of torque required to achieve the states. Thus, by utilizing inverse dynamic model or a feedforward system in the controller, there will be an estimation for the required torque that the actuators can apply to achieve the states. However, the analytical model has some noise due to the modeling error that can be minimized by using a low pass filter. In this study, a low pass filter with a cutoff frequency of 30 Hz was used to minimize the noise in the output of the feedforward network. The Simulink model of the inverse dynamics system along with the low pass filter is shown in Figure 4.

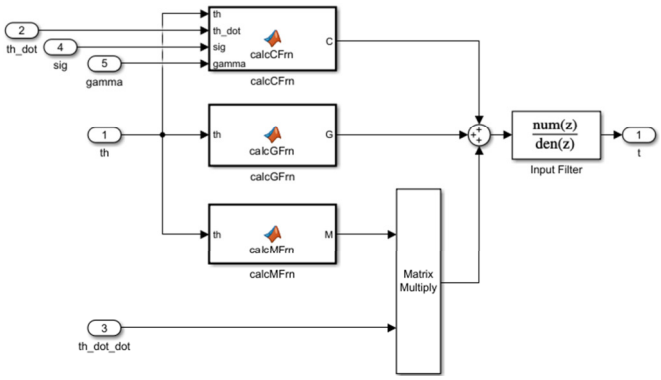

Fig. 4. Feedforward system (inverse dynamics of the robot).

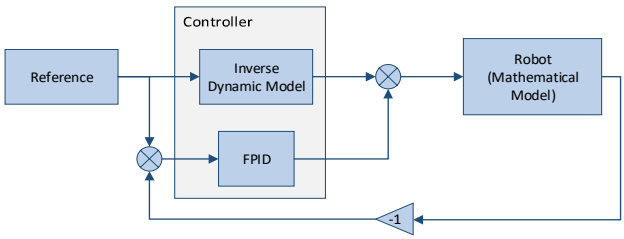

Fig. 5. Block diagram of the feedforward and FOPID controllers.

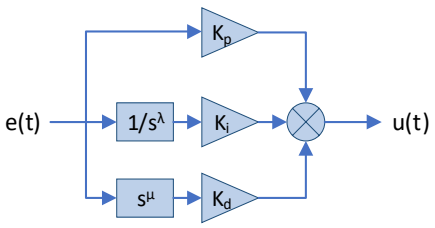

Fig. 6. Block diagram of the FOPID.

The block diagram of the system is presented in Figure 5Fig. 5. , where the controller consists of a feedforward system and the FOPID. The robot input is a summation of the output states of the feedforward model and the FOPID compensator. The FOPID compensator is illustrated in Figure 6. It can be seen that the controller consists of the three gains (K_p, K_i, and K_d), and a fractional order integral and a fractional order derivative having order λ and μ respectively. As the integral order of the PID compensator, the input provided to the system shown in Figure 6 is the error signal $e(t)$ and the output is the controller output referred to as $u(t)$.

A. *Controller Tunning*

In order to tune the two additional parameters for the non-integer order controller, the ABC algorithm is used, which is a algorithm inspired by nature [19], applied to optimize a large set of testing functions. This optimization method has been used to tune different controller applications for different system plants as well. In this study, the ABC method is used to tune the FOPID and the Integral Order PID (IoPID) controllers, where the tuning parameters are $[P \quad I \quad D \quad \lambda \quad \mu]$ for FOPID and $[P \quad I \quad D \quad N]$ for IOPID, λ is the order of the integral, μ is the order of the derivative, and N is the derivative filter used in IOPID. The cost function minimization is used for tuning. In this regard, the cost function shown in (11) was considered:

$$fit = [W_1 \quad W_2 \quad W_3 \quad W_4 \quad W_5]\begin{bmatrix} T_s \\ M_o \\ e_{ss} \\ u(t) \\ \sum t \cdot |e(t)| \end{bmatrix} \qquad (11)$$

where W_n is a weight vector that can be assigned manually in the algorithm to specify the importance of a specific entity in the fitness value, T_s is the settling time, M_o is the overshoot, e_{ss} is the setting error, $u(t)$ is the input signal of the plant, and $e(t)$ is the difference between the reference and the output signals: $e(t) = r(t) - y(t)$.

TABLE II. CONTROLLER PARAMETERS AFTER TUNING WITH ABC

Type	Parameter	Joint 1	Joint 2	Joint 3
IoPID	*P*	45.0986	33.5967	-169.5471
	I	16.1521	37.1599	-445.3873
	D	27.7447	10.4947	-65.7642
	N	5997.6464	6522.7668	84023.2904
FoPID	*P*	180	480.7269	-170.7471
	I	60.3385	295.8896	-140.4873
	D	40.8152	100.0941	-35.1754
	λ	0.83	0.697	0.837
	μ	0.75	0.68	0.85

The incorporation of weights in the fitness function for calculating fitness values offers significant advantages in the parameter estimation process. By assigning different weights to various performance criteria, such as settling time, error, or other system-specific metrics, the relative importance of all the parameters can effectively be controlled during the optimization process. This approach provides flexibility in fine-tuning the behavior of the system. One can prioritize certain criteria that are more critical for the specific application or align with the desired control objectives. For example, if achieving a fast-settling time is of utmost importance, a higher weight can be assigned to settling time in the fitness function. On the other hand, if minimizing steady-state error is the primary concern, a higher weight can be assigned to the error term. This allows us to strike a balance between conflicting objectives and tailor the control system's behavior according to

specific requirements. The tuned controller values can be seen in Table II.

IV. SIMULATION RESULTS AND DISCUSSION

The simulation environment used for this study is shown in Figure 7, where the integral and fractional controllers are used to control the manipulator's states in task space. For both control methods, the same plant model is used, i.e. a fractional dynamic model to incorporate the performance test of each controller and compare them without any difficulty.

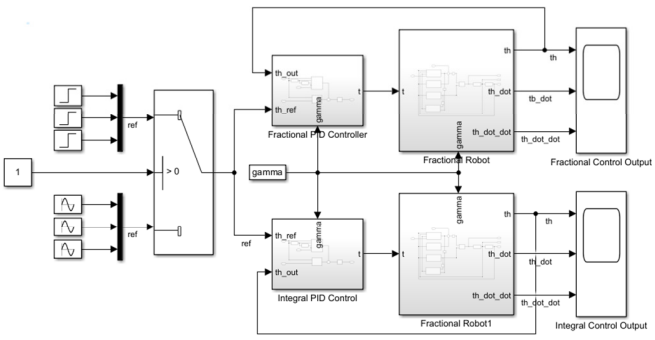

Fig. 7. Simulation environment block diagram with plant and controllers.

There are two types of reference inputs used in this simulation. A step input is used to analyze the output step response of the system and a sinusoidal input is used to analyze the tracking response of the system in the task space. The reference input can be selected using a switch for the ease where false (0) corresponds to sinusoidal reference and true (1) to step reference inputs. The step input signal is demonstrated in Figure 8.

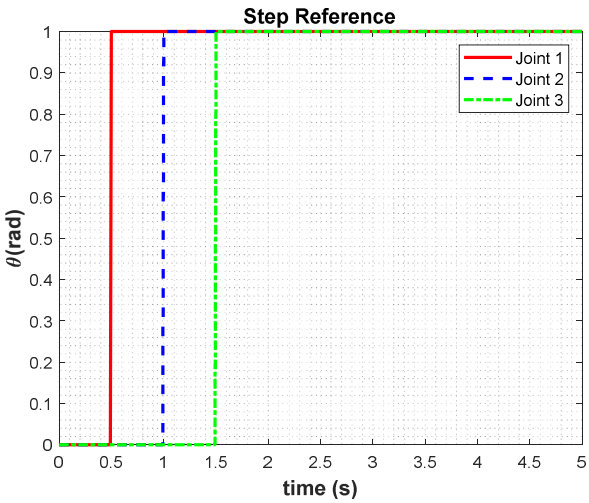

Fig. 8. Step reference input used in the simulations.

To assess the controllers' capability to counter disturbances, a disturbance step input of -8 Nm magnitude is applied to both controllers (IOPID and FOPID) at each joint. This scenario can be linked to the sudden impact of a strong wind gust on a delicate mechanism. During this simulation, akin to the transient effects of wind, a predefined counter torque is exerted on each joint of the robotic arm. The disturbance input, symbolizing the abrupt nature of a wind gust, is initiated precisely at 3 s into the simulation, remains active for a duration of 1 s, and is then deactivated as shown in Figure 9, where a step having a magnitude of -8 Nm is used and again a step to 0 Nm after 1 s. This approach allows us to scrutinize the manipulators response to this disruptive force and its subsequent recovery.

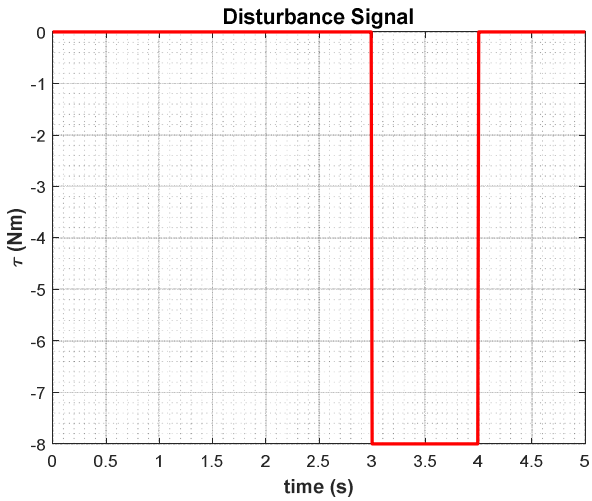

Fig. 9. Disturbance input signal (wind gust for 1 s).

In the context of this research, where the aim is to scrutinize the output performance of the FOPID and IOPID controllers applied to a fractional order plant model of a robotic manipulator, a simulation environment was meticulously crafted. This environment served as the crucible for comparing the response of both controllers in the presence of a step input used as a reference signal. Figure 10 shows a visual representation of the simulation output, which shows a difference between the output response of the IOPID and FOPID controllers. Each joint of the robotic manipulator underwent a calculated step response, the portrayal of which can be observed in Figure 8. The step response of a system gives enough information to analyze the control behavior of the structure. Figure 10 lays the foundation for a comprehensive analysis, where we engaged in a juxtaposition of the performances exhibited by the FOPID and IOPID controllers. Upon embarking on a visual examination of the output results shown in Figure 10, a recurrent theme emerges with striking clarity: the FOPID controller consistently outshines its integer order counterpart across a multitude of performance metrics. This encompasses crucial aspects like settling time, rise time, overshoot, and steady-state error. As the data unfolds, a pattern of excellence surfaces, one that reaffirms the efficacy of the fractional order control approach in the realm of robotic manipulator precision and stability. Also, in Figure 10, it can be seen that the reference input, as shown in Figure 8 was applied for both controllers based on the articulated robotic arm model, where the step was applied at different times for each joint in order to ensure the stability of the robot due the inertial effect of the dynamic system.

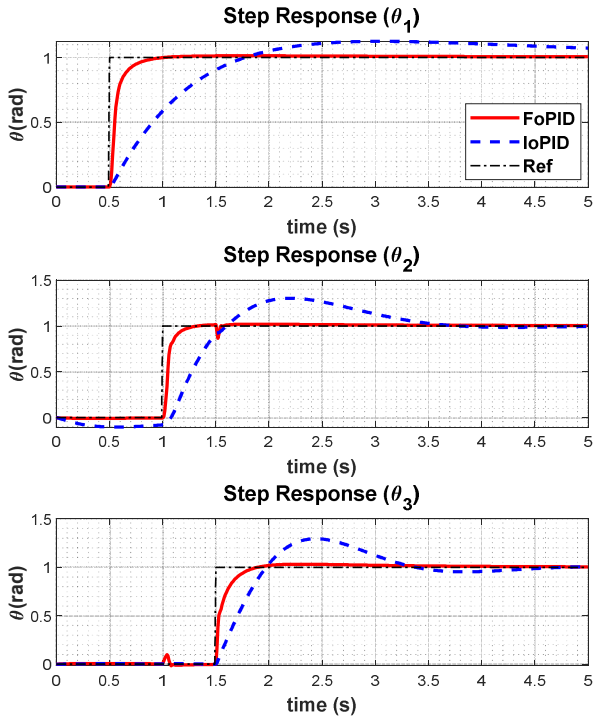

Fig. 10. A comparison of the step output response of the integral and fractional controllers in the task space.

Using Figure 10, Table III was developed, where the necessary performance parameters are described. Table III helps to analyze the performance of both controllers in the time domain. To ensure a meticulous and transparent presentation of our findings, the quantified values for each performance metric are thoughtfully organized. This tabulation provides readers a panoramic view of the comprehensive spectrum of performance outcomes, which shows that the FOPID controller stands as a beacon of improvement, boasting an enhancement exceeding 50% when compared with its IOPID counterpart.

TABLE III. FOPID-IOPID RESULT COMAPRISON

Parameters (Joint 3)	IoPID	FoPID
Rise time (s)	0.51	0.26
Settling time (s)	3.1	1.5
Overshoot (%)	30	3
Undershoot (%)	0	0
Stead state error	0	0
Peak	1.3	1.03

These findings, gleaned from an intricate interplay of simulation, analysis, and meticulous observation, shed light on the transformative potential of the fractional order control methodologies within the realm of robotic manipulator dynamics. This substantiates the foundation for our comparative study and heralds new horizons in the advancement of control paradigms.

The impact of the disturbance is vividly illustrated in Figure 11, showcasing the disturbance output. Upon examining the response of both controllers, a distinctive disparity becomes apparent: the FOPID controller exhibits a subdued response to the disturbance, actively attempting to counteract its effects. Conversely, the IOPID controller experiences a pronounced perturbation due to the disturbance, significantly affecting the system's behavior. This contrast is particularly noticeable when scrutinizing the response of joint 2, as clearly depicted in Figure 11. The FOPID controller's ability to mitigate the disturbance's impact is evident, with the response maintaining a more stable trajectory. In stark contrast, the disturbance's disruptive effect on the IOPID controller's response is readily observable. These findings not only underscore the robust disturbance rejection capability of the FOPID controller, but also emphasize the challenges that the IOPID controller faces when confronted with disturbances. Such insights further enhance our comprehension of the controllers' efficacy in maintaining stability and precision under varying external influences.

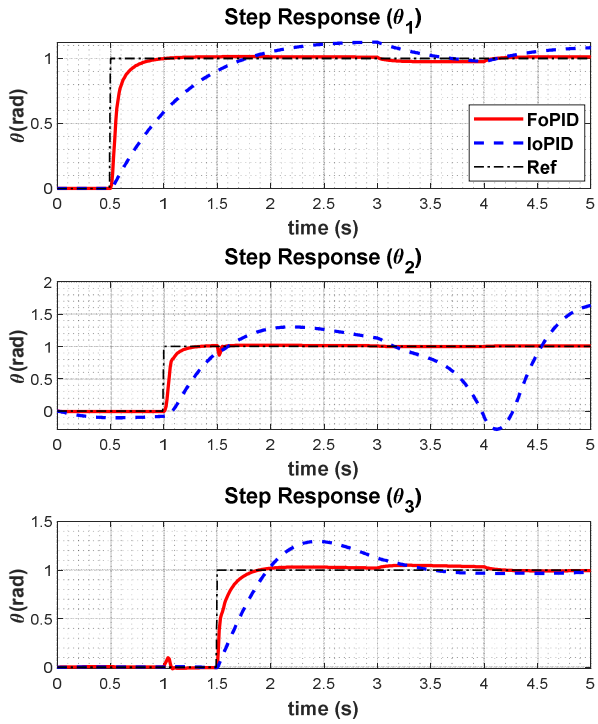

Fig. 11. A comparison of the step output response of integral and fractional controllers in the task space.

V. CONCLUSION

In this paper, a fractional (non-integer) order robotic arm system has been modeled in order to identify the system parameters more accurately. For the kinematics modeling of the system and for the kinetics or dynamics, the DH-method and the Euler-Lagrange method were employed, respectively. With the fractional order system model, a fractional order controller was applied to the robotic arm system. It was shown that with the proposed system identification and the proposed fractional controller, which adds two additional tuning parameters (λ and μ) to the controller, system position and stability improved. Robotic arm position control accuracy is a critical task and can be challenging with system disturbances and uncertainty and with the proposed FOPID controller the

system was able to maintain its positioning stability and provide an improved time response with or without the presence of environmental disturbances in the system. The FoPID controller was compared to the integer order controller, and the simulation results verify that the proposed non-integer order controller outperforms the integer order controller and provides overall lower overshoot and settling time along with improving the system time response in achieving the desired position.

ACKNOWLEDGMENT

This work was supported and funded by the Deanship of Scientific Research at Imam Mohammad Ibn Saud Islamic University (IMSIU) (grant number IMSIU-RG23039).

REFERENCES

[1] M. Bi, "Control of Robot Arm Motion Using Trapezoid Fuzzy Two-Degree-of-Freedom PID Algorithm," *Symmetry*, vol. 12, no. 4, Apr. 2020, Art. no. 665, https://doi.org/10.3390/sym12040665.

[2] A. Ashagrie, A. O. Salau, and T. Weldcherkos, "Modeling and control of a 3-DOF articulated robotic manipulator using self-tuning fuzzy sliding mode controller," *Cogent Engineering*, vol. 8, no. 1, Jan. 2021, Art. no. 1950105, https://doi.org/10.1080/23311916.2021.1950105.

[3] N. Tan, P. Yu, Z. Zhong, and F. Ni, "A New Noise-Tolerant Dual-Neural-Network Scheme for Robust Kinematic Control of Robotic Arms With Unknown Models," *IEEE/CAA Journal of Automatica Sinica*, vol. 9, no. 10, pp. 1778–1791, Oct. 2022, https://doi.org/10.1109/JAS.2022.105869.

[4] J. Iqbal, "Modern Control Laws for an Articulated Robotic Arm: Modeling and Simulation," *Engineering, Technology & Applied Science Research*, vol. 9, no. 2, pp. 4057–4061, Apr. 2019, https://doi.org/10.48084/etasr.2598.

[5] C. Relaño, J. Muñoz, C. A. Monje, S. Martínez, and D. González, "Modeling and Control of a Soft Robotic Arm Based on a Fractional Order Control Approach," *Fractal and Fractional*, vol. 7, no. 1, Jan. 2023, Art. no. 8, https://doi.org/10.3390/fractalfract7010008.

[6] L. Zouari, S. Chtourou, M. B. Ayed, and S. A. Alshaya, "A Comparative Study of Computer-Aided Engineering Techniques for Robot Arm Applications," *Engineering, Technology & Applied Science Research*, vol. 10, no. 6, pp. 6526–6532, Dec. 2020, https://doi.org/10.48084/etasr.3885.

[7] D. Nicolis, F. Allevi, and P. Rocco, "Operational Space Model Predictive Sliding Mode Control for Redundant Manipulators," *IEEE Transactions on Robotics*, vol. 36, no. 4, pp. 1348–1355, Dec. 2020, https://doi.org/10.1109/TRO.2020.2974092.

[8] J. O. Pedro and T. Tshabalala, "Hybrid NNMPC/PID control of a two-link flexible manipulator with actuator dynamics," in *2015 10th Asian Control Conference (ASCC)*, Kota Kinabalu, Malaysia, Feb. 2015, https://doi.org/10.1109/ASCC.2015.7244737.

[9] M. I. Ullah, S. A. Ajwad, M. Irfan, and J. Iqbal, "MPC and H-Infinity Based Feedback Control of Non-Linear Robotic Manipulator," in *2016 International Conference on Frontiers of Information Technology (FIT)*, Islamabad, Pakistan, Sep. 2016, pp. 136–141, https://doi.org/10.1109/FIT.2016.033.

[10] A. Tepljakov, *Fractional-order Modeling and Control of Dynamic Systems*. Springer International Publishing, 2017.

[11] M. W. Spong, S. Hutchinson, and M. Vidyasagar, *Robot Modeling and Control*, 1st ed. Hoboken, NJ, USA: Wiley, 2005.

[12] H. S. Lafmejani and H. Zarabadipour, "Modeling, Simulation and Position Control of 3 Degree of Freedom Articulated Manipulator," *Indonesian Journal of Electrical Engineering and Informatics (IJEEI)*, vol. 1, no. 3, pp. 99–108, Sep. 2013, https://doi.org/10.52549/ijeei.v1i3.80.

[13] J. E. Escalante-Martínez *et al.*, "Fractional differential equation modeling of viscoelastic fluid in mass-spring-magnetorheological damper mechanical system," *The European Physical Journal Plus*, vol. 135, no. 10, Oct. 2020, Art. no. 847, https://doi.org/10.1140/epjp/s13360-020-00802-0.

[14] J. F. Gómez-Aguilar, H. Yépez-Martínez, C. Calderón-Ramón, I. Cruz-Orduña, R. F. Escobar-Jiménez, and V. H. Olivares-Peregrino, "Modeling of a Mass-Spring-Damper System by Fractional Derivatives with and without a Singular Kernel," *Entropy*, vol. 17, no. 9, pp. 6289–6303, Sep. 2015, https://doi.org/10.3390/e17096289.

[15] N. Sene and J. F. Gómez Aguilar, "Fractional Mass-Spring-Damper System Described by Generalized Fractional Order Derivatives," *Fractal and Fractional*, vol. 3, no. 3, Sep. 2019, Art. no. 39, https://doi.org/10.3390/fractalfract3030039.

[16] S. Manjaree and M. Thomas, "Modeling of Multi-DOF Robotic Manipulators using Sim-Mechanics Software," *Indian Journal of Science and Technology*, vol. 9, no. 48, Dec. 2016, https://doi.org/10.17485/ijst/2016/v9i48/105833.

[17] R. Abdulkader, "Controller Design based on Fractional Calculus for AUV Yaw Control," *Engineering, Technology & Applied Science Research*, vol. 13, no. 2, pp. 10432–10438, Apr. 2023, https://doi.org/10.48084/etasr.5687.

[18] R. Abdulkader, "Proportional-Integral Controller based on Fractional Calculus for a Microgrid System," in *2023 International Conference on Fractional Differentiation and Its Applications (ICFDA)*, Ajman, United Arab Emirates, Mar. 2023, https://doi.org/10.1109/ICFDA58234.2023.10153154.

[19] D. Karaboga, "An Idea Based on Honey Bee Swarm for Numerical Optimization," Erciyes University, Kayseri, Türkiye, Technical Report TR06, Oct. 2005.